

A Wireless Near-Infrared Spectroscopy Device for Flap Monitoring: Proof of Concept in a Porcine Musculocutaneous Flap Model

Changsheng Wu, PhD^{1,*} Alina Y. Rwei, PhD^{1,2,*} Jong Yoon Lee, BSE^{1,3}  Wei Ouyang, PhD¹ Lauren Jacobson, MD⁴ Haixu Shen, BSE, MS⁵ Haiwen Luan, PhD¹ Yameng Xu, BSE, MS⁶ Jun Bin Park, BS³ Sung Soo Kwak, PhD¹ Xiaoyue Ni, PhD¹ Wubin Bai, PhD⁵ Daniel Franklin, PhD¹ Shuo Li, PhD¹ Yiming Liu, BSE⁷ Xinchen Ni, PhD¹ Amanda M. Westman, PhD⁴ Matthew R. MacEwan, MD, PhD⁶ John A. Rogers, PhD^{1,5,7,8,9,10,11} Mitchell A. Pet, MD⁴ 

¹Department of Materials Science and Engineering, Querrey Simpson Institute for Bioelectronics, Northwestern University, Chicago, Illinois

²Department of Chemical Engineering, Delft University of Technology, Delft, The Netherlands

³Sibel Inc., Evanston, Illinois

⁴Division of Plastic and Reconstructive Surgery, Department of Surgery, School of Medicine, Washington University, St. Louis, Missouri

⁵Department of Materials Science and Engineering, Northwestern University, Evanston, Illinois

⁶Department of Neurosurgery, School of Medicine, Washington University, St. Louis, Missouri

⁷Department of Electrical and Computer Engineering, Northwestern University, Evanston, Illinois

⁸Department of Mechanical Engineering, Northwestern University, Evanston, Illinois

Address for correspondence Mitchell A. Pet, MD, Division of Plastic and Reconstructive Surgery, Department of Surgery, School of Medicine, Washington University, 660 S. Euclid Avenue, St. Louis, MO 63110 (e-mail: mpet@wustl.edu).

John A. Rogers, PhD, Department of Materials Science and Engineering, Northwestern University, 2145 Sheridan Road, Evanston, IL 60208 (e-mail: jrogers@northwestern.edu).

⁹Department of Biomedical Engineering, Northwestern University, Evanston, Illinois

¹⁰Department of Chemistry, Northwestern University, Evanston, Illinois

¹¹Department of Neurological Surgery, Feinberg School of Medicine, Northwestern University, Chicago, Illinois

J Reconstr Microsurg 2022;38:96–105.

Abstract

Background Current near-infrared spectroscopy (NIRS)-based systems for continuous flap monitoring are highly sensitive for detecting malperfusion. However, the clinical utility and user experience are limited by the wired connection between the sensor and bedside console. This wire leads to instability of the flap–sensor interface and may cause false alarms.

Methods We present a novel wearable wireless NIRS sensor for continuous fasciocutaneous free flap monitoring. This waterproof silicone-encapsulated Bluetooth-enabled device contains two light-emitting diodes and two photodetectors in addition to a battery sufficient for 5 days of uninterrupted function. This novel device was compared with a ViOptix T.Ox monitor in a porcine rectus abdominus myocutaneous flap model of arterial and venous occlusions.

Results Devices were tested in four flaps using three animals. Both devices produced very similar tissue oxygen saturation (StO₂) tracings throughout the vascular clamping events, with obvious and parallel changes occurring on arterial clamping, arterial

Keywords

- ▶ tissue perfusion monitoring
- ▶ near-infrared spectroscopy
- ▶ flap monitoring

* These authors contributed equally to this study.

received

March 29, 2021

accepted after revision

May 12, 2021

published online

August 17, 2021

© 2021, Thieme. All rights reserved.
Thieme Medical Publishers, Inc.,
333 Seventh Avenue, 18th Floor,
New York, NY 10001, USA

DOI <https://doi.org/10.1055/s-0041-1732426>.
ISSN 0743-684X.

release, venous clamping, and venous release. Small interdevice variations in absolute StO₂ value readings and magnitude of change were observed. The normalized cross-correlation at zero lag describing correspondence between the novel NIRS and T.Ox devices was >0.99 in each trial.

Conclusion The wireless NIRS flap monitor is capable of detecting StO₂ changes resultant from arterial vascular occlusive events. In this porcine flap model, the functionality of this novel sensor closely mirrored that of the T.Ox wired platform. This device is waterproof, highly adhesive, skin conforming, and has sufficient battery life to function for 5 days. Clinical testing is necessary to determine if this wireless functionality translates into fewer false-positive alarms and a better user experience.

Microsurgical free flap reconstruction of oncologic, traumatic, and congenital defects requires microvascular anastomosis to establish perfusion of the transferred tissue. As these anastomoses are susceptible to thrombosis in the postoperative period, flap tissue perfusion monitoring is imperative. The duration of flap monitoring varies with surgeon and institution, but traditionally free flaps are monitored for 3 to 5 days prior to hospital discharge.¹

Current strategies for cutaneous free flap monitoring are variable. Traditional intermittent methods such as serial physical examination and external Doppler are limited by their inherently subjective nature and requirement for skilled bedside personnel. Additionally, intermittent assessment strategies are subject to delays in the detection of malperfusion because clear external signs of flap malperfusion may take several hours to become obvious.² Internal Doppler systems³⁻⁵ position a wired Doppler probe directly at or adjacent to the anastomosis, and provide a continuous audible signal which is indicative of blood flow. While this may accelerate the process of identifying a malperfused flap and improve flap salvage rate,^{6,7} these systems are not well suited to remote monitoring and still require frequent attendance by skilled personnel at bedside. Furthermore, these systems have a high rate of false-positive alarms due to probe disengagement,^{8,9} and may cause direct deformation of or trauma to the anastomosis during placement and/or removal.^{5,7,8}

Recently, near-infrared spectroscopy (NIRS) has gained favor as a strategy for continuous monitoring of cutaneous free flaps.^{7,9} This technology is noninvasive and provides objective data which facilitates remote monitoring and reduces the need for skilled personnel at bedside. The T.Ox device (ViOptix Inc., Fremont, CA) is a widely utilized NIRS-based monitor which has demonstrated excellent sensitivity and specificity for the detection of flap compromise.⁹

In our practice, we have found the T.Ox system to have many desirable clinical characteristics, but it is still subject to some limitations. The T.Ox system includes a cable connection between the probe and external display console which is necessary for the functionality of its infrared (IR) light-emitting lasers, and for the transmission of the gathered data back to the bedside display. Unfortunately, shifts in patient position, rearrangement of linens, or attempts at

ambulation which cause even modest traction on or twisting of this cable frequently result in disturbance of or fluid incursion into the flap-probe interface. These events often generate spurious signal change or loss which necessitates immediate sensor/cable troubleshooting or replacement and undue worry for the surgeon and patient.^{10,11} These false alarms can also infrequently result in unnecessary emergent surgical exploration which exposes patients to additional risk and increases the cost of care.

In this article, we introduce a self-contained Bluetooth-enabled totally wireless NIRS probe. This device is waterproof, highly adhesive, skin conforming, and has sufficient battery life to continuously monitor a flap for up to 5 days. Performance of this device is evaluated in a head-to-head comparison with the T.Ox system in a porcine rectus abdominus myocutaneous flap model of arterial and venous compromise.

Methods

Wireless NIRS Probe

The wireless NIRS sensor introduced here is flexible, waterproof, lightweight, and has a robust nonirritant adhesive skin interface. ►Fig. 1A, B presents top and bottom views of the device, and ►Fig. 1C, D shows a detailed exploded-view schematic illustration of the device.

Bluetooth low energy technology is used to remotely monitor tissue oxygenation through measurement of back-scattered light from the tissue. The electronic subsystems include (1) 740 nm red light-emitting diode (LED; QBHP684, QT Brightek) and 860 nm IR LED (SFH 4059, OSRAM Opto Semiconductors) as the light sources for spectroscopy; (2) two PIN photodiodes (PDs) at distances of 5 and 10 mm from the LEDs for detecting the backscattered light intensities; (3) a microcontroller (nRF52832, Nordic Semiconductor) for controlling the LEDs, acquiring signals from the PDs and communicating the data wirelessly; and (4) a 150-mAh battery to support 5 days of continuous operation. These electronics are mounted on a flexible printed circuit board that includes a 75- μ m-thick polyimide middle layer and two patterned 18- μ m-thick polyimide copper layers on top and bottom surfaces.

The LED and PD subsystems form the sensing module (2.5 cm \times 2 cm) and the microcontroller and battery

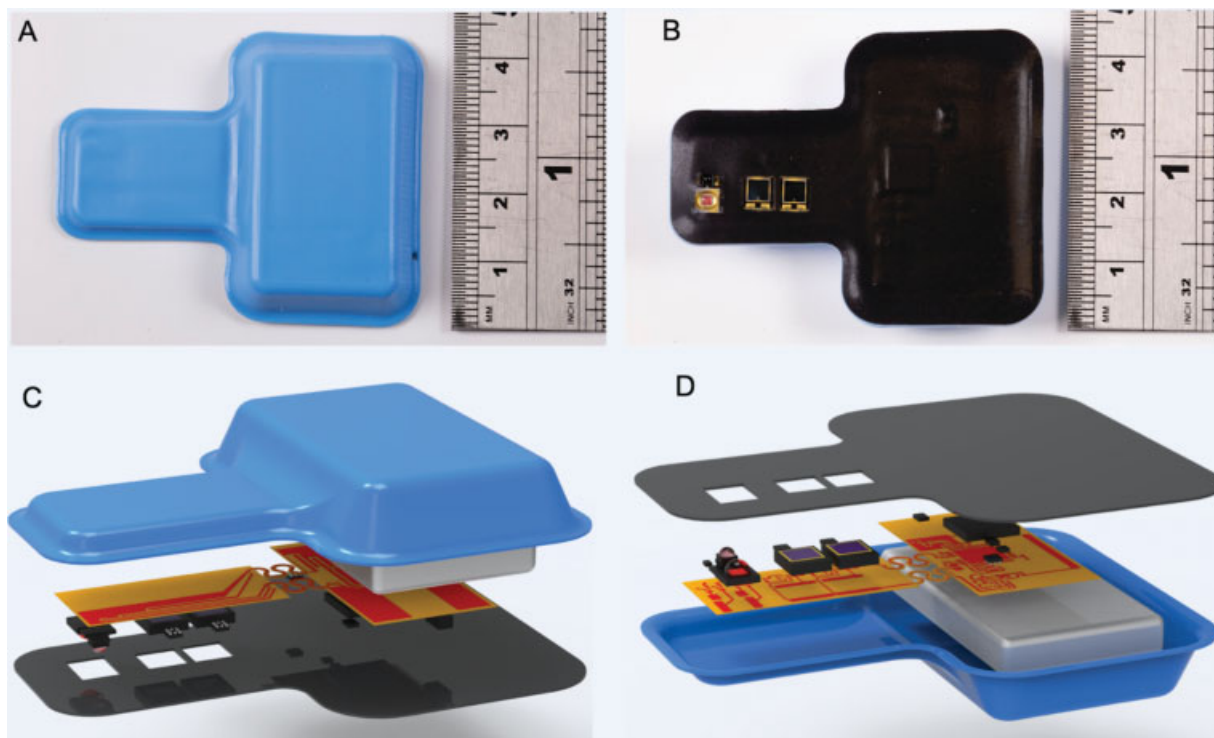


Fig. 1 The wireless near-infrared spectroscopy sensor is depicted photographically from top (A) and bottom (B), and using an exploded CAD rendering from the top (C) and bottom (D). CAD, Computer Aided Design.

subsystems constitute the control module (2.7 cm × 4.3 cm). Serpentine interconnects¹²⁻¹⁴ join the two sections and mechanically isolate the thin (2.2 mm), low-modulus sensing module from the thicker (6.6 mm), control module. The device is encapsulated in a skin-safe silicone elastomer (Silbione RTV 4420, Elkem Silicones) and a thin medical silicone tape (2477P, 3M) facilitates attachment to nonplanar skin tissue even during motion. The device weighs ~11 g.

During operation, the red and IR LEDs activate alternately at 25 Hz and with a 1% duty cycle. The microcontroller acquires signals from the two PDs and then initiates transmission of them to a smartphone or tablet for data logging, analysis, and display. The average current consumption of the device is 0.84 mA. A custom-developed app with algorithms based on spatially resolved spectroscopy (SRS),^{15,16} calculates and displays a tissue oxygen saturation (StO₂) index every 10 seconds. SRS can determine the absolute concentrations of oxyhemoglobin (HbO₂) and deoxyhemoglobin (HHb),¹⁷ and thus lead to the calculation of StO₂. The Bluetooth range is ~30 feet, and the device is designed to automatically reconnect if the signal is obstructed or if the device temporarily moves out of range.

Porcine Model

Animal research was performed with approval of the Institutional Animal Care and Use Committee at Washington University School of Medicine. This was performed as per U.S. Department of Agriculture Animal Welfare Regulations at an accredited facility. One live pig was utilized for this study. Anesthesia was induced with Telazol, ketamine, and xylazine followed by maintenance with inhaled isoflurane. After

completion of all experimentations, the animal was euthanized with pentobarbital.

A pedicled rectus abdominus myocutaneous flap was raised based on the deep superior epigastric artery and veins in addition to the superficial superior epigastric vein. This flap harvest procedure was adapted from Bodin et al.¹⁸ After elevation, flap viability was confirmed by visualization of bright red bleeding at the entire periphery.

Experimental Design

Wireless NIRS probe and a ViOptix T.Ox probe were adhered to the central portion of the flap. The T.Ox probe was attached to the external monitor via the fiberoptic cable, and Bluetooth connection was established between the wireless NIRS device and an iPad running the monitoring application (► Fig. 2). The flap was monitored continuously throughout the experiment using both devices in parallel.

After achieving a stable baseline reading for 10 minutes, an Acland clamp was applied to the deep superior epigastric artery to induce complete ischemia. Ischemia was maintained for 15 minutes (► Fig. 3A). The Acland clamp was then released and 15 minutes were then allowed for flap recovery and re-establishment of a stable baseline reading (► Fig. 3B). Acland clamps were then applied to the bilateral deep and superficial superior epigastric veins to induce venous congestion (► Fig. 3C). Congestion was maintained for 15 minutes. The Acland clamps were then released and 15 minutes were then allowed for flap recovery and re-establishment of a stable baseline reading (► Fig. 3D). The experiment was then immediately repeated two or three additional times using the same flaps.

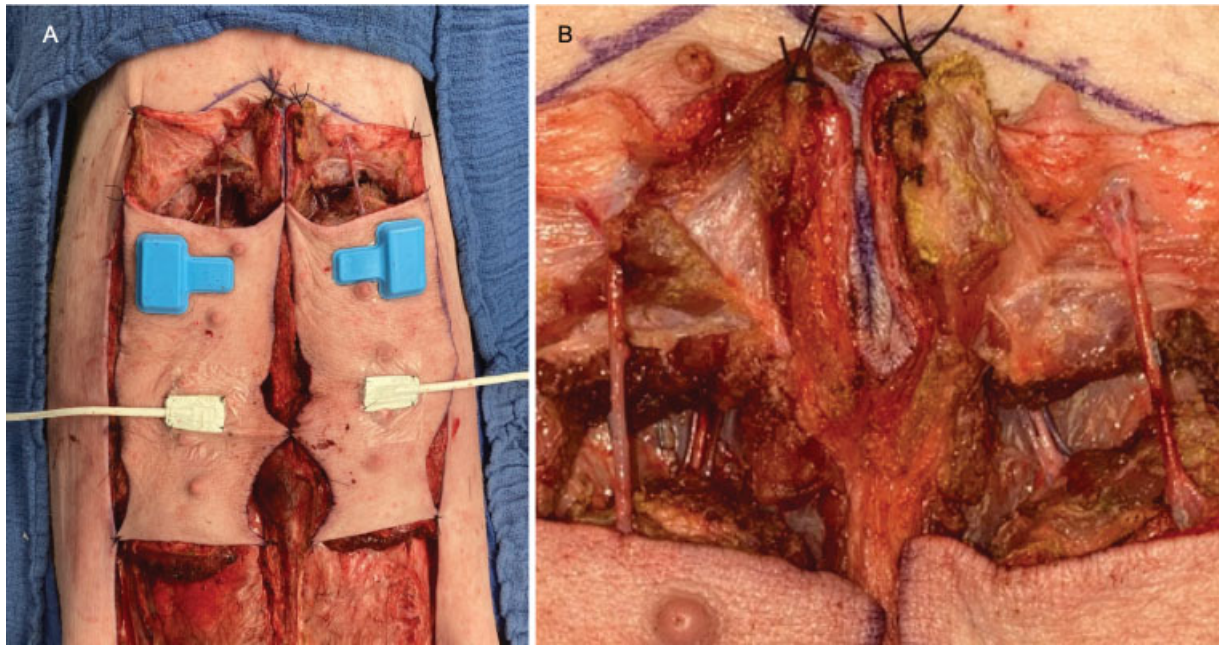


Fig. 2 (A) Bilateral porcine rectus abdominus myocutaneous flaps based on the deep superior epigastric vessels and the superficial superior epigastric vein. (B) Closeup view of the flap pedicle vessels. The deep superior epigastric artery and venae comitans are deeper and closer to midline, while the superficial superior epigastric vein is more lateral and superficial.

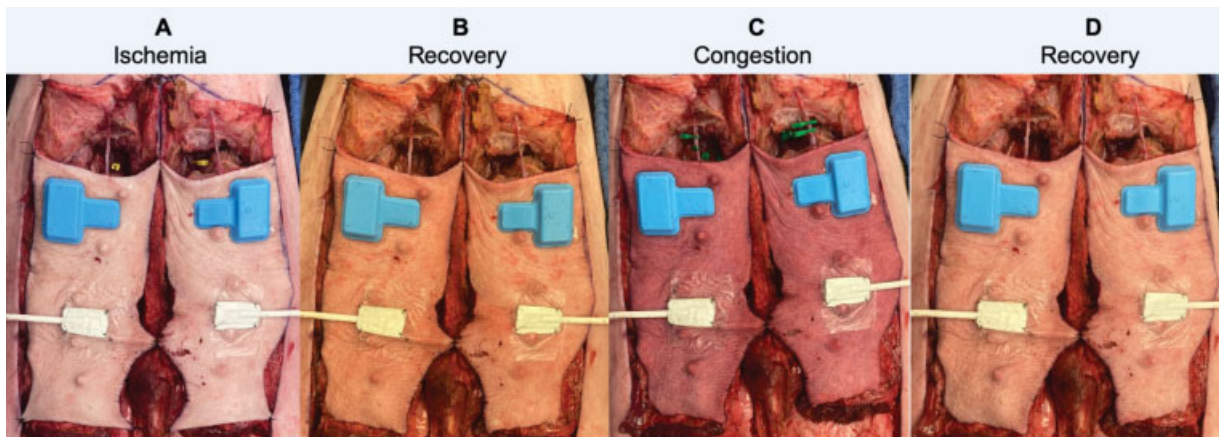


Fig. 3 After achievement of a stable baseline, each cycle of testing consisted sequentially of 15 minutes of ischemia (A), 15 minutes of recovery (B), 15 minutes of venous congestion (C), and then an additional 15 minutes of recovery (D).

StO₂ Calculation

SRS measures the light reflectance at different distances and estimates the absorption and scattering properties of the tissue based on the diffusion approximation. The detailed derivation of the solution to the diffusion equation governing the lighting propagation in the tissue can be found elsewhere.^{15–17} The spatial derivative of absorbance enables the estimation of absorption coefficients,

$$\dot{\lambda}_a(\ddot{e}) = \frac{1}{3\dot{\lambda}'_s} \left(\ln(10) \frac{\partial A(\ddot{e})}{\partial \ddot{n}} - \frac{2}{\ddot{n}} \right)^2$$

where $\dot{\lambda}_a$ is the absorption coefficient, $\dot{\lambda}'_s$ is the reduced scattering coefficient, and \ddot{n} is the distance between the

LED source and the center of the two PDs. The absorption coefficients directly correlate with hemoglobin concentrations as follows:

$$\begin{bmatrix} c_{\text{HHb}} \\ c_{\text{HbO}_2} \end{bmatrix} = \frac{1}{\ln(10)} \begin{bmatrix} \dot{a}_{\text{HHb},\ddot{e}1} & \dot{a}_{\text{HbO}_2,\ddot{e}1} \\ \dot{a}_{\text{HHb},\ddot{e}2} & \dot{a}_{\text{HbO}_2,\ddot{e}2} \end{bmatrix}^{-1} \begin{bmatrix} \dot{\lambda}_{a,\ddot{e}1} \\ \dot{\lambda}_{a,\ddot{e}2} \end{bmatrix}$$

where c is the chromophore concentration and \dot{a} is the specific molar extinction coefficient. The tissue oxygenation index is then calculated as

$$\text{StO}_2 = \frac{c_{\text{HbO}_2}}{c_{\text{HbO}_2} + c_{\text{HHb}}}$$

Statistical Methods

Normalized cross-correlation at zero lag was used to describe the correspondence between the wireless NIRS and T.Ox sensors being compared.

Results

This experiment was successfully performed in three animals, using a total of four flaps. In the first animal, bilateral flaps were raised and bilateral simultaneous head-to-head trials were performed. In the second animal, two novel devices (in addition to T.Ox) were tested simultaneously on a single flap to highlight consistency between devices. In the third animal, a single flap and a single device were tested. The ischemic and congested conditions were successfully achieved and recovered using the protocol earlier, as confirmed by the expected changes in flap color (►Fig. 3A–D) and StO₂. Continuous monitoring was accomplished using both devices throughout each cycle of ischemia and congestion. We encountered no instances of wireless (novel device)

or wired (T.Ox) connection loss during any experiment. Both devices produced very similar StO₂ tracings throughout the vascular clamping events, with precipitous changes occurring on arterial clamping, arterial release, venous clamping, and venous release. The T.Ox and wireless NIRS tracings for the right and left flaps in Animal 1 are shown in ►Figs. 4 and 5, respectively. The T.Ox and two simultaneous independent wireless NIRS tracings from Animal 2 are shown in ►Fig. 6. The T.Ox and wireless NIRS tracings from Animal 3 are shown in ►Fig. 7. Small interdevice variations in absolute StO₂ value readings and magnitude of change were observed. The normalized cross-correlation at zero lag describing correspondence between the wireless NIRS and T.Ox devices ranged from 0.992 to 0.998. The normalized cross-correlation at zero lag describing correspondence between the two wireless NIRS which simultaneously monitored the flap in Animal 2 was 0.997. Each of these values reflects the aggregate correspondence of the thousands of parallel StO₂ measurements taken over the course of each experiment.

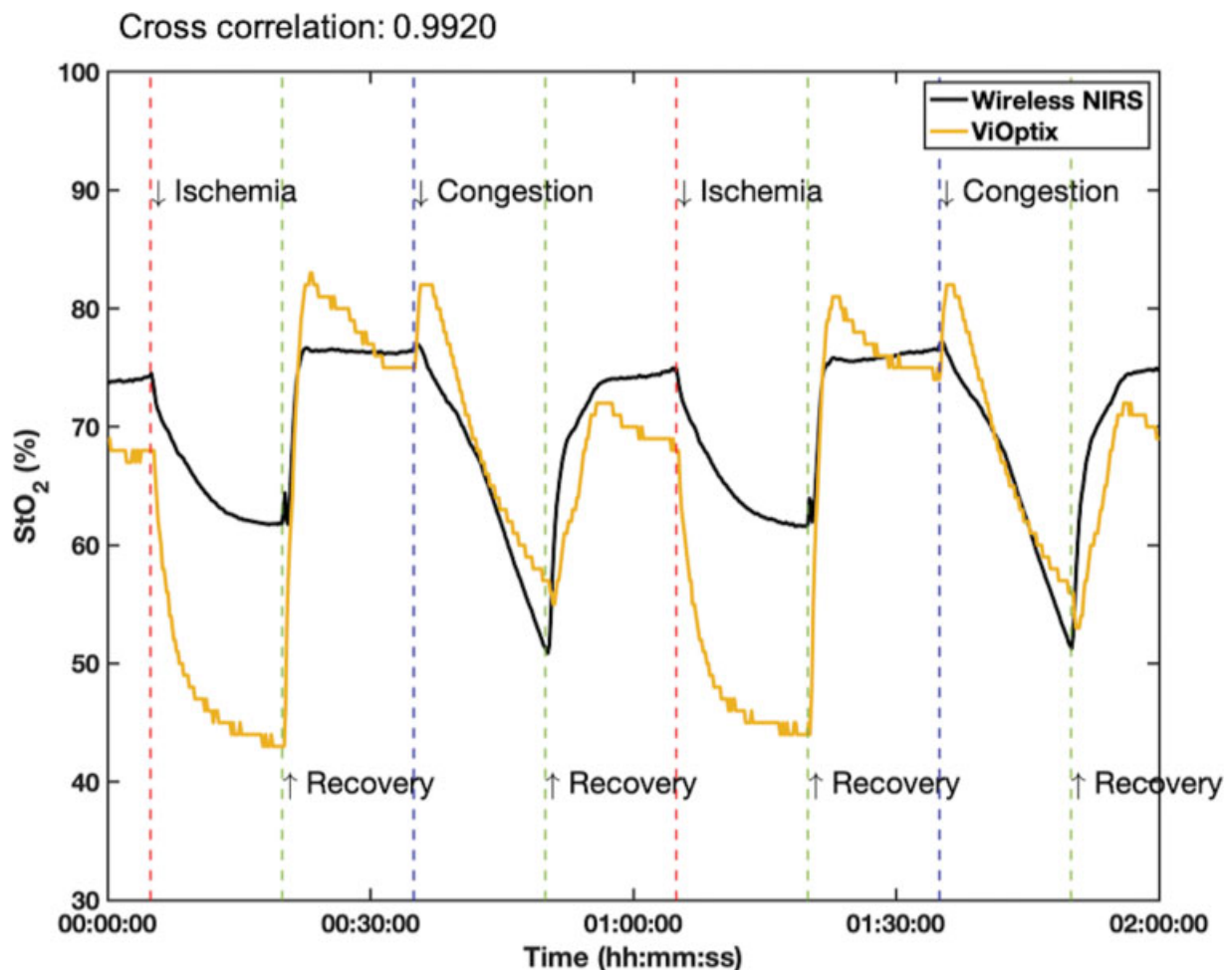


Fig. 4 Animal 1, right flap; T.Ox (yellow, lighter tracing) and wireless NIRS tracing (black). This graph shows three cycles of continuous testing. The tracings begin with a baseline, and then the flap is made ischemic (red line). After 15 minutes, the arterial clamp is removed (green line) and the flap is allowed to recovery for 15 minutes. The veins are then clamped (blue line) to achieve the congested state, and then released 15 minutes later (green line). After an additional 15 minutes of recovery back to baseline, the cycles is repeated two more times. NIRS, near-infrared spectroscopy.

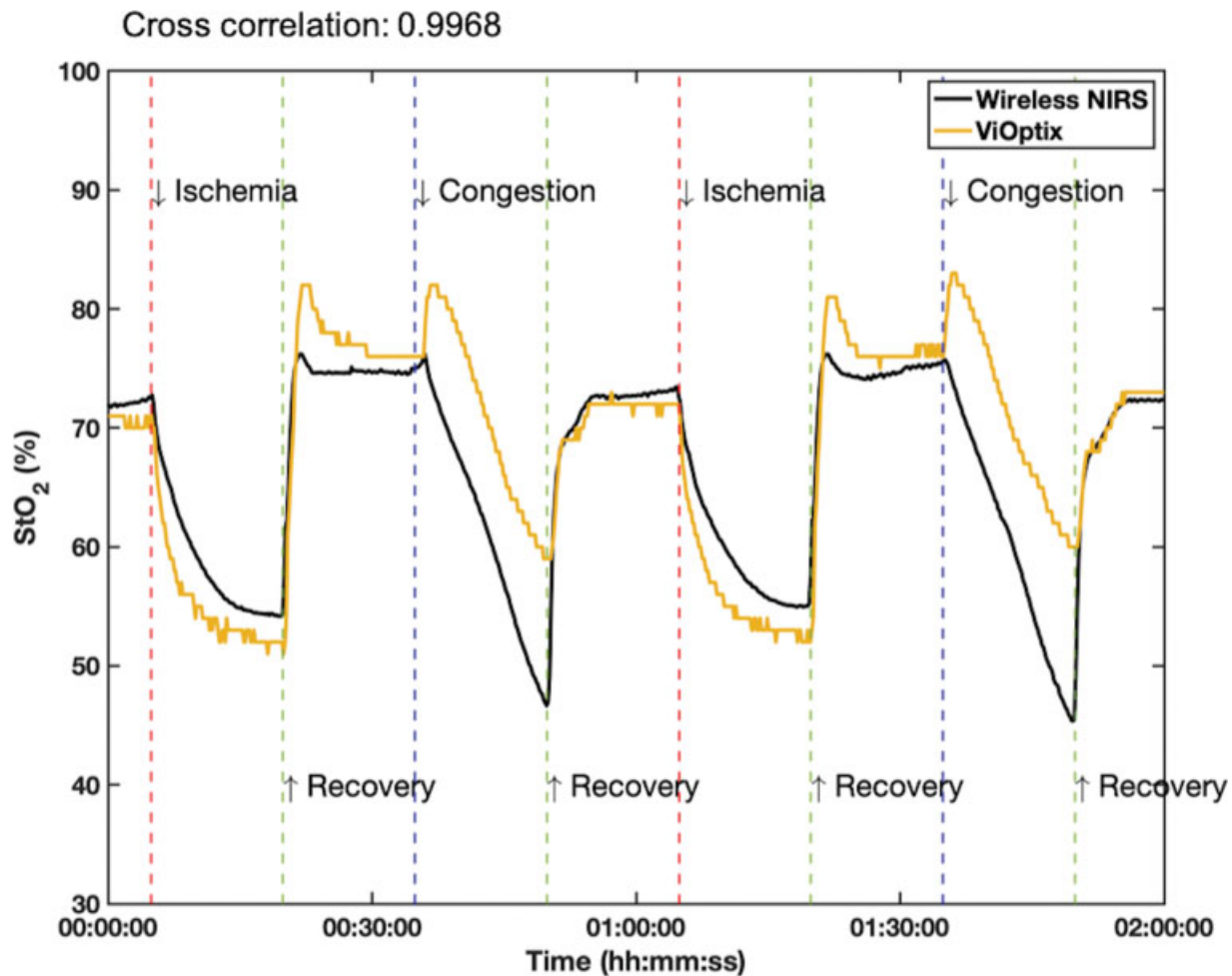


Fig. 5 Animal 1, left flap; T.Ox (yellow, lighter tracing) and wireless NIRS tracing (black). This graph shows three cycles of continuous testing. NIRS, near-infrared spectroscopy.

Discussion

Prior Innovations for Wireless Continuous Flap Monitoring

NIRS entails the transcutaneous application of light in the near-IR spectrum. As oxygenated and deoxygenated hemoglobin have differential absorption at the selected wavelengths, this method can assess their relative concentrations and thereby measure tissue oxygen saturation. This paradigm has several advantages, perhaps the most important of which is that it is deployed on the cutaneous paddle in a location remote from the delicate flap pedicle. Furthermore, given that the output (StO₂) is numeric and objective, the requirement for bedside personnel is reduced, and remote monitoring is facilitated.

The T.Ox device (ViOptix Inc.) has proven to be a useful clinical tool but its limitations have been noted by several authors,^{10,11} and are well known to any nurse or resident routinely tasked with using the device. In addition to being cumbersome and restricting patient positioning and ambulation, even minimal traction on the thick fiberoptic cable connecting the flap probe to the bedside display can generate spurious signal change or loss. This occurs by partial or complete delamination of the probe from the flap skin,

with or without incursion of blood or other fluid. This may occur many times over the course of a day, and each instance requires immediate flap examination with troubleshooting or replacement of the probe.¹⁰ These repeated episodes are very stressful for the patient, surgeon, house staff, and nurses, and contribute to some surgeon's hesitation to adopt this technology.

This clinical problem has spurred the proposal of several potential wireless solutions. These include a totally implantable Doppler system,^{19–21} and an implantable biodegradable arterial pressure sensor which is able to detect flow across the arterial pedicle vessel.^{22,23} These innovations represent a potential improvement upon the familiar Cook-Swartz Doppler²⁴ which requires a wired connection between the vascular cuff and the bedside device. However, both of these devices retain a common key disadvantage. As each device directly encircles the anastomotic vessels, vascular damage, kinking, or constriction may occur during or after device placement.^{5,8,25}

Recognizing the benefits of a peripheral NIRS-based monitoring strategy, Berthelot et al developed the first wireless sensor to utilize NIRS technology for the purpose of flap monitoring.^{26–28} The device developed by this group utilizes two LEDs of differing wavelengths and a single PD.

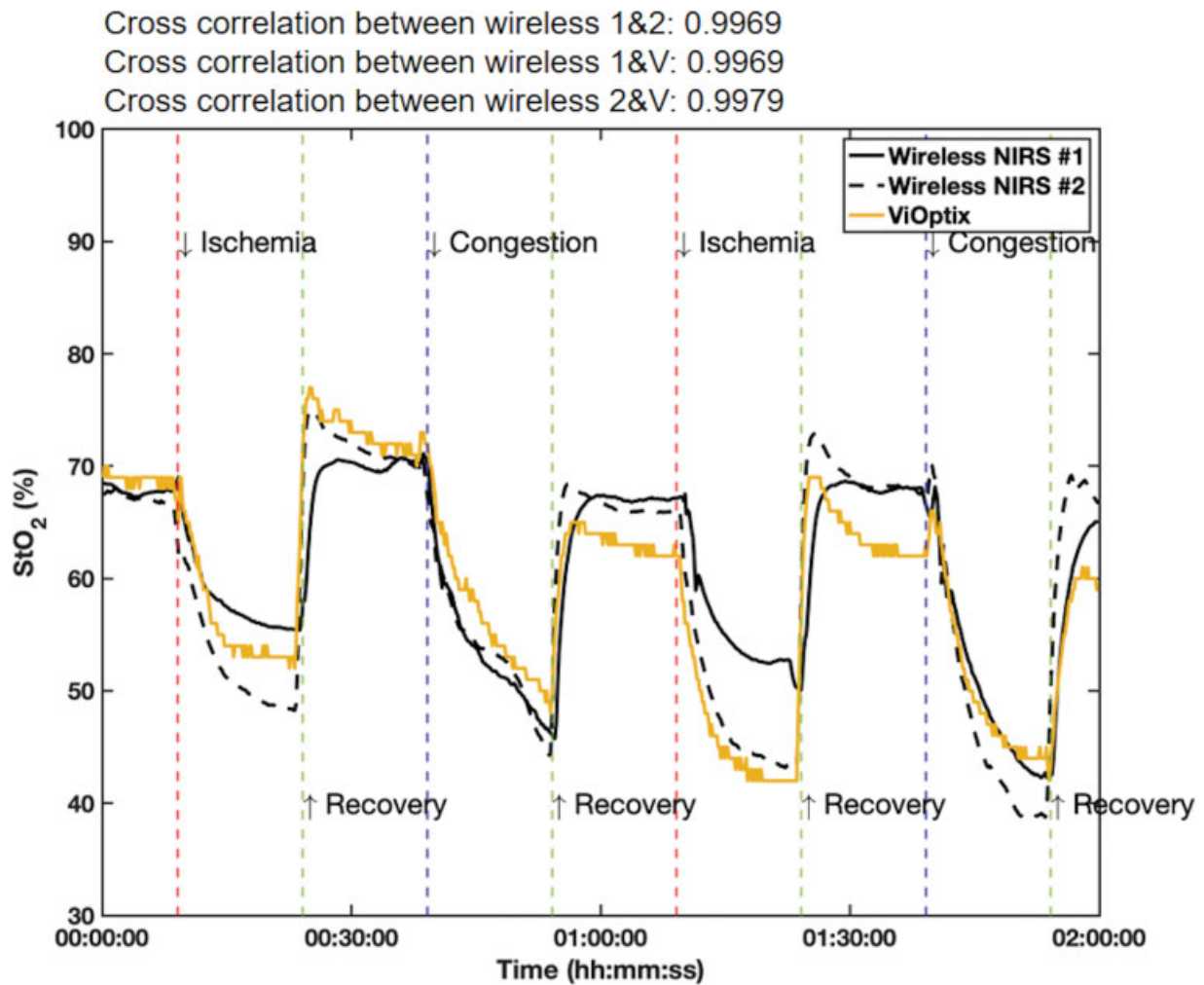


Fig. 6 Animal 2; T.Ox (yellow lighter solid tracing), wireless NIRS tracing 1 (solid black), wireless NIRS tracing 2 (dotted black). In this graph, the T.Ox device and two wireless NIRS sensors are used to monitor flap perfusion over two cycles of baseline/ischemia/recovery/congestion/recovery. NIRS, near-infrared spectroscopy.

This design yields data that support analysis based on DS, which can only lead to an estimation of StO₂ by use of nontrivial assumptions of light scattering losses in the tissue and the introduction of additional error-correcting factors. Specifically, their methodology takes tissue-dependent absorption and scattering coefficients as preassumed constants²⁹ which affect the accuracy of StO₂ measurement and hinders the deployment on different flaps. Our design with two PDs, on the other hand, enables SRS analysis and thus derivation of tissue absorption coefficients directly from measured optical densities.

Furthermore, battery lifetime and sampling rate represent additional parameters that are important to the continuous and timely monitoring of flaps in clinical settings. Battery lifetime of 30 to 40 hours and a sampling rate of 0.25 Hz for the previously reported device may not satisfy clinical needs. These systems also rely on conventional rigid circuit boards and hard plastic enclosures that can frustrate soft, conformal adhesion to the skin. While this represents a significant advance of providing NIRS with a wireless platform, it does not replicate the clinical utility of the T.Ox device, and direct comparisons of

their wireless sensor to clinical standard systems were not reported.

Novel Wireless NIRS Device

Here, we introduce a wireless NIRS device for peripheral monitoring of flap perfusion. While conceptually similar to the T.Ox system, this novel device utilizes self-contained LEDs instead of external fiberoptically transmitted laser light, and replaces the hard-wired connection between probe and processor with Bluetooth connectivity. Devoid of any external tether, this device will be less susceptible to the spurious signal changes and losses caused by patient movement or wire traction. Beyond eliminating the cable, additional features to stabilize the flap-probe interface have been included. Flexible electronics within a silicone housing enable this sensor to not only conform to the curves of any flap but also accommodate the contour changes that occur with position changes. Furthermore, the device is mounted on the skin using a water-resistant silicone adhesive which is sturdy and will completely exclude fluid from the flap-probe interface.

StO₂ readings are recorded every 10 seconds and transmitted wirelessly to a bedside smartphone or tablet running

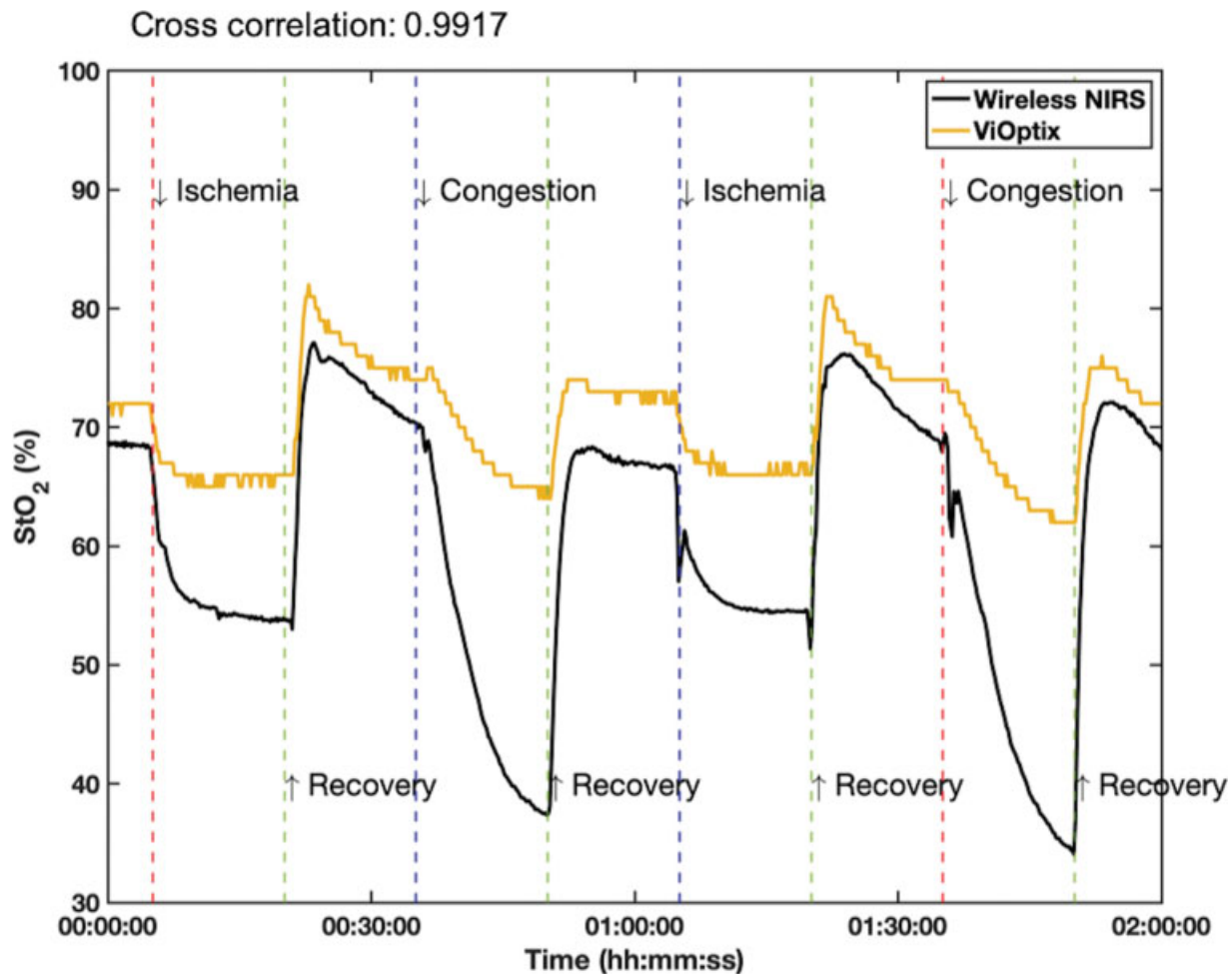


Fig. 7 Animal 3; T.Ox (yellow lighter tracing), wireless NIRS tracing 1 (black). In this graph, the T.Ox device and a wireless NIRS sensor are used to monitor flap perfusion over two cycles of baseline/ischemia/recovery/congestion/recovery. NIRS, near-infrared spectroscopy.

an app-based display which also supports remote monitoring. Each disposable probe has a materials cost <\$100 and there is no need for a proprietary console display module, which eliminates the need for the \$25,000 to \$30,000 of capital expenditure per unit.^{7,11,30} The device is powered by an internal lithium polymer battery which can function for 5 days in the absence of external power supply or battery recharging/replacement. In addition to including battery protection and power management circuits, the battery is encased in water proof stretchable silicone materials to ensure that the device is safe and shelf stable. With a diminutive size of 53 × 43 × 6.6 mm and 11 g, this device can be worn comfortably and without obstructing a large portion of the flap.

Head-to-Head Comparison of Wireless NIRS Device and T.Ox

To demonstrate that the wireless NIRS device can replicate StO₂ sensing functionality of the T.Ox device, the two devices were compared head to head in a porcine rectus abdominus myocutaneous flap model. Altogether, the experiment was conducted five times using four flaps in three live animals. After mounting both sensors in adjacent positions on the same flap, conditions of arterial and venous anastomotic

thromboses were simulated by occluding the flap artery or veins. We found that both the T.Ox and wireless NIRS monitors showed immediate and precipitous drops in the StO₂ tracing upon arterial or venous occlusion, and prompt increases upon release of the clamps. Throughout all trials, the StO₂ curves for the two monitors closely mirrored each other, and cross-correlations at zero lag time were uniformly above 0.99. In one experiment (Animal 2), two novel wireless sensors were used (in addition to T.Ox) to monitor the flap, and excellent agreement (cross-correlation >0.99) between these two devices was observed.

Small interdevice variations in absolute StO₂ value and magnitude of change were observed. These are attributable to the fact that the monitors were positioned adjacent to each other on flaps, and monitored slightly different areas of tissue. While each was exposed to the same macroderangements in blood flow, local intraflap variability of perfusion, and StO₂ is expected, and is often observed clinically. Small differences in sensor application, light intensity, and encapsulation materials (e.g., elastomer thickness) may also play a role. Despite these variations, the congruent response of the wireless NIRS and T.Ox sensors to vascular occlusion was unmistakable, and we believe that the matched StO₂ curves would have been interpreted identically in a clinical setting.

Study Strengths, Limitations, and Future Work

Strengths of this study include the utilization of a large-animal flap model which is anatomically and physiologically very similar to abdominal flaps that are routinely performed in humans. As the wireless NIRS and T.Ox sensors were tested simultaneously on the same flap, direct performance comparison was facilitated. Furthermore, sensor testing in three animals, using four flaps, over a total of 20 vascular occlusive events demonstrates that our results are consistent and replicable.

Limitations of this study include that this was a pedicled flap model wherein vascular occlusion was accomplished with Acland clamps rather than anastomotic thrombosis as it would occur in a free flap. Performance of these devices in a partial vascular occlusion model has not yet been assessed. Additionally, given that this was a nonsurvival animal model, testing could only be performed on the animal while under anesthesia, and over a period of hours rather than days. Given this limitation, it is important to recognize that while we have made an argument that this novel wireless NIRS device will lead to a reduction in false alarms and improved patient/surgeon experience, this hypothesis has not yet been tested nor proven. While only four flaps in three animals were used in this proof of concept study, we felt that additional animal experiments were not justified and have elected to devote future resources to human clinical trials.

Finally, the wireless prototype devices tested required slightly different scattering coefficients for data analysis. This likely represents minor variations in device construction and encasement which is currently done by hand. Furthermore, estimations of tissue StO₂ using both devices require several assumptions about the light scattering properties of heterogeneous tissues. This is reflected in the wide range of T.Ox derived apparent StO₂ values which can characterize a healthy flap. Further efforts will focus on calibration of our device with gold-standard measures of blood oxygenation to increase the precision of NIRS-based measurements.

In future studies, wireless NIRS device will be clinically tested in parallel with the standard-of-care T.Ox device in human free tissue transfers. This will allow assessment of durability and longevity (of the device and adhesive interface) in the clinical environment, and allow us to test the hypothesis that this novel device has equal capability to detect flap malperfusion, with enhanced resistance to spurious readings and false alarms.

Conclusion

We have introduced a self-contained wireless NIRS-based device for continuous StO₂ monitoring of cutaneous free flaps. This device is waterproof, highly adhesive, skin conforming, and has sufficient battery life to function for 5 days. This device interfaces with any smartphone or tablet at bedside, and requires no additional equipment. Head-to-head testing of this device and the standard-of-care T.Ox system in a porcine rectus abdominus myocutaneous flap model revealed nearly identical performance in conditions of flap ischemia and congestion. This device is ready for translation into human subjects where further testing is necessary

to assess its performance and potential benefits in the clinical setting.

Funding

Funding for this study was received from the Division of Plastic Surgery and the Department of Neurosurgery at Washington University, and from the Querry Simpson Institute of Bioelectronics at Northwestern University.

Conflict of Interest

M.M.M. has no potential or actual conflict of interest related to the present study or subject matter. M.M.M. holds an equity position in Acera Surgical, Inc. and Osteo-Vantage, Inc., is a board member at Acera Surgical, Inc., and has received funding from ConductiveBio, Inc. M.A.P. has no potential or actual conflict of interest related to the present study or subject matter. M.A.P. has received research funding from Checkpoint Inc. Other authors have no actual or potential conflict of interest.

References

- 1 Harashina T, Fujino T, Watanabe S. The intimal healing of microvascular anastomoses. *Plast Reconstr Surg* 1976;58(05):608–613
- 2 Chao AH, Meyerson J, Povoski SP, Kocak E. A review of devices used in the monitoring of microvascular free tissue transfers. *Expert Rev Med Devices* 2013;10(05):649–660
- 3 Rozen WM, Enajat M, Whitaker IS, Lindkvist U, Audolfsson T, Acosta R. Postoperative monitoring of lower limb free flaps with the Cook-Swartz implantable Doppler probe: a clinical trial. *Microsurgery* 2010;30(05):354–360
- 4 Guillemaud JP, Seikaly H, Cote D, Allen H, Harris JR. The implantable Cook-Swartz Doppler probe for postoperative monitoring in head and neck free flap reconstruction. *Arch Otolaryngol Head Neck Surg* 2008;134(07):729–734
- 5 Zhang T, Dyalram-Silverberg D, Bui T, Caccamese JF Jr, Lubek JE. Analysis of an implantable venous anastomotic flow coupler: experience in head and neck free flap reconstruction. *Int J Oral Maxillofac Surg* 2012;41(06):751–755
- 6 Rozen WM, Chubb D, Whitaker IS, Acosta R. The efficacy of postoperative monitoring: a single surgeon comparison of clinical monitoring and the implantable Doppler probe in 547 consecutive free flaps. *Microsurgery* 2010;30(02):105–110
- 7 Berthelot M, Ashcroft J, Boshier P, et al. Use of near-infrared spectroscopy and implantable Doppler for postoperative monitoring of free tissue transfer for breast reconstruction: a systematic review and meta-analysis. *Plast Reconstr Surg Glob Open* 2019;7(10):e2437–e2438
- 8 Paydar KZ, Hansen SL, Chang DS, Hoffman WY, Leon P. Implantable venous Doppler monitoring in head and neck free flap reconstruction increases the salvage rate. *Plast Reconstr Surg* 2010;125(04):1129–1134
- 9 Kagaya Y, Miyamoto S. A systematic review of near-infrared spectroscopy in flap monitoring: current basic and clinical evidence and prospects. *J Plast Reconstr Aesthet Surg* 2018;71(02):246–257
- 10 Inbal A, Song DH. Discussion: does increased experience with tissue oximetry monitoring in microsurgical breast reconstruction lead to decreased flap loss? The learning effect. *Plast Reconstr Surg* 2016;137(04):1102–1103
- 11 Koelen PGL, Vargas CR, Ho OA, et al. Does increased experience with tissue oximetry monitoring in microsurgical breast reconstruction lead to decreased flap loss? The learning effect. *Plast Reconstr Surg* 2016;137(04):1093–1101

- 12 Xu S, Zhang Y, Jia L, et al. Soft microfluidic assemblies of sensors, circuits, and radios for the skin. *Science* 2014;344(6179):70–74
- 13 Chung HU, Rwei AY, Hourlier-Fargette A, et al. Skin-interfaced biosensors for advanced wireless physiological monitoring in neonatal and pediatric intensive-care units. *Nat Med* 2020;26(03):418–429
- 14 Lee K, Ni X, Lee JY, et al. Mechano-acoustic sensing of physiological processes and body motions via a soft wireless device placed at the suprasternal notch. *Nat Biomed Eng* 2020;4(02):148–158
- 15 Suzuki S, Takasaki S, Ozaki T, Kobayashi Y. Tissue oxygenation monitor using NIR spatially resolved spectroscopy. In: Chance B, Alfano RR, Tromberg BJ, eds. *Optical Tomography and Spectroscopy of Tissue III*. Vol. 3597. SPIE Proceedings. International Society for Optics and Photonics 1999:582–592
- 16 Matcher SJ, Kirkpatrick PJ, Nahid K, Cope M, Delpy DT. Absolute quantification methods in tissue near-infrared spectroscopy. In: Chance B, Alfano RR, eds. *Optical Tomography, Photon Migration, and Spectroscopy of Tissue and Model Media: Theory, Human Studies, and Instrumentation*. Vol. 2389. SPIE Proceedings International Society for Optics and Photonics; 1995:486–495
- 17 Lindkvist M, Granåsen G, Grönlund C. Coherent derivation of equations for differential spectroscopy and spatially resolved spectroscopy: an undergraduate tutorial. *Spectrosc Lett* 2013;46(04):243–249
- 18 Bodin F, Diana M, Koutsomanis A, Robert E, Marescaux J, Bruant-Rodier C. Porcine model for free-flap breast reconstruction training. *J Plast Reconstr Aesthet Surg* 2015;68(10):1402–1409
- 19 Rothfuss MA, Franconi NG, Unadkat JV, et al. A system for simple real-time anastomotic failure detection and wireless blood flow monitoring in the lower limbs. *IEEE J Transl Eng Health Med* 2016;4:4100114
- 20 Unadkat JV, Rothfuss M, Mickle MH, Sejdic E, Gimbel ML. The development of a wireless implantable blood flow monitor. *Plast Reconstr Surg* 2015;136(01):199–203
- 21 Rothfuss MA, Unadkat JV, Gimbel ML, Mickle MH, Sejdic E. Totally implantable wireless ultrasonic Doppler blood flowmeters: toward accurate miniaturized chronic monitors. *Ultrasound Med Biol* 2017;43(03):561–578
- 22 Oda H, Beker L, Kaizawa Y, et al. A novel technology for free flap monitoring: pilot study of a wireless, biodegradable sensor. *J Reconstr Microsurg* 2020;36(03):182–190
- 23 Boutry CM, Beker L, Kaizawa Y, et al. Biodegradable and flexible arterial-pulse sensor for the wireless monitoring of blood flow. *Nat Biomed Eng* 2019;3(01):47–57
- 24 Chang EI, Ibrahim A, Zhang H, et al. Deciphering the sensitivity and specificity of the implantable Doppler probe in free flap monitoring. *Plast Reconstr Surg* 2016;137(03):971–976
- 25 Anctil V, Brisebois S, Fortier P-H. Free flap anastomosis leak after implantable Doppler removal. *OTO Open* 2017;1(01):X17697057
- 26 Berthelot M, Yang G-Z, Lo B. A self-calibrated tissue viability sensor for free flap monitoring. *IEEE J Biomed Health Inform* 2018;22(01):5–14
- 27 Berthelot M, Henry FP, Hunter J, et al. Pervasive wearable device for free tissue transfer monitoring based on advanced data analysis: clinical study report. *J Biomed Opt* 2019;24(06):1–8
- 28 Berthelot M, Chen C-M, Yang G-Z, Lo B. Wireless wearable self-calibrated sensor for perfusion assessment of myocutaneous tissue. In: *IEEE*; 2016:171–176
- 29 Chen CM, Kwasnicki R. Wearable tissue oxygenation monitoring sensor and a forearm vascular phantom design for data validation. In: *2014 11th International Conference on Wearable and Implantable Body Sensor Networks*. 2014
- 30 Kozusko S, Gbulie U. Detecting microsurgical complications with ViOptix tissue oximetry in a pediatric myocutaneous free flap: case presentation and literature review. *J Reconstr Microsurg Open* 2018;03(01):e8–e12